JOURNAL OF MATERIALS SCIENCE 20 (1985) 1637–1644

On the optical properties of Mn/SiO and SiO thin films

S. K. J. AL-ANI, M. A. R. SARKAR, J. BEYNON, C. A. HOGARTH
Department of Physics, Brunel University, Uxbridge, Middlesex, UK

The ultraviolet, visible and infrared properties of unannealed and annealed amorphous Mn/SiO cermet thin films (300 to 1000 nm thick) prepared by vacuum evaporation at 5.0×10^{-4} Pa are investigated. The ultraviolet and visible results are analysed assuming optical absorption by indirect transitions. A systematic reduction of the optical energy gap and an increase in the width of the band-tail region is observed with increasing metallic content. The effects of the ratio deposition rate/residual pressure and substrate temperature on the optical properties of SiO_x $(1 < x < 2)$ thin films are also investigated.

1. Introduction

The study of optical absorption spectra with photon energy as the main variable, and temperature, pressure and electric field as secondary variables, provides essential information on phonon and electron states in a material, whether it be crystalline, amorphous or liquid. In an amorphous material, long-range order is destroyed, and, certain sharp well-defined features, such as the fundamental absorption edge, which are observed in the optical spectra of crystals disappear. However, the main features of the absorption spectra will be broadly similar [1] if the short-range order in the amorphous material is roughly the same as that in a crystalline material of the same chemical composition.

The absorption coefficient $\alpha(\omega)$ in the high absorption region ($> 10^4$ cm^{-1}) is given by [2, 3]:

$$\alpha(\omega) = B(\hbar\omega - E_{opt})^2/\hbar\omega \qquad (1)$$

where ω is the angular frequency of the radiation, $\hbar$ is Planck's constant h divided by 2π, E_{opt} is the optical energy gap and B is a constant equal to $4\pi\sigma_0/cnE_e$, where σ_0 is the electrical conductivity extrapolated to absolute zero, E_e is the width of the tails of localized states in the band gap region and n is the refractive index. A graph of $\{\alpha(\omega)\hbar\omega\}^{1/2}$ against $\hbar\omega$ gives E_{opt} as the intercept produced on the $\hbar\omega$ axis by the linear portion of the graph and $B^{1/2}$ as the gradient. Equation 1 offers the best fit for the optical absorption data in many oxides and chalcogenide glasses [4, 5]. It has also been successfully applied to the absorption edge in some amorphous oxide films [6, 7].

For $\alpha < 10^4$ cm^{-1}, the relation

$$\alpha(\omega) = \alpha_0 \exp(\hbar\omega/E_e) \qquad (2)$$

often holds. Here α_0 is a constant. This relation was first proposed by Urbach [8] to describe the absorption edge in alkali halide crystals. Although Equation 2 is applicable to many amorphous materials, the precise mechanism involved is not established with certainty.

In recent years there has been an increasing interest in ceramic–metal (cermet or granular metal) and discontinuous thin films because of their many potential applications [9, 10]. A cermet thin film is characterized by three different structural regions [11]. These are:

1. metallic: in this regime the volume fraction of metal is large and the island separation is small, thus generating a metallic matrix with dielectric inclusions. The temperature coefficient of resistance (TCR) is positive, but may be negative if voids or other defects are present;

2. dielectric: the structure is an inversion of (1) with small metal particles dispersed in a dielectric matrix; the TCR is negative;

3. transitional: the structure is intermediate between (1) and (2) and consists of metallic filaments and isolated islands. The exact compo-

0022–2461/85 $03.00 + .12

sition of the onset of this regime seems to depend on the deposition conditions.

A variety of cermet systems has been studied, e.g. Cr/SiO [12, 13], Au/SiO [14, 15] and Mn/SiO [16–19]. There are many aspects of their conduction mechanism which requires further investigation.

In this paper an investigation of some optical properties (E_{opt}, n and infrared absorption peaks) of Mn/SiO cermets and SiO_x films is reported. The influence of the deposition parameters on the optical properties is also discussed.

2. Experimental techniques

Mn/SiO and SiO_x thin films were deposited on clean Corning 7059 glass substrates, held at fixed temperatures between 20 and 300° C, by thermal evaporation at a total residual pressure of 5.0×10^{-4} Pa in an Edwards coating plant (model: E19A3). The cermet films were prepared by evaporating appropriate mixes of manganese (Koch-light Ltd) and silicon oxide (Union Carbide Ltd) powders from a single tantalum boat. The ratio of deposition rate, R, to residual pressure, P, was varied between 7.5×10^2 and 9.0×10^3 nm sec^{-1} Pa^{-1} and the film thickness varied between 300 and 1050 nm. A quartz crystal monitor (Edwards: model FTM2) controlled the deposition rate and multiple beam interferometry was used to estimate the film thickness. Specimens for both of the optical studies were prepared simultaneously.

Optical absorption measurements in the wavelength range 190 to 850 nm were carried out at 20° C using a Perkin–Elmer spectrophotometer (model 402). After correcting for reflection at the first surface, $\alpha(\omega)$ was calculated from the absorbance, A, and film thickness, d, using the relation

$$\alpha(\omega) = 2.303\, A/d. \qquad (3)$$

The refractive index, n, was estimated using the equation [20]

$$(1/2nd) = (1/\lambda_2 - 1/\lambda_1) \qquad (4)$$

where λ_1 and λ_2 are the wavelengths of adjacent transmission maxima in the A against λ curve.

Specimens for the infrared absorption study in the range 4000 to 200 cm^{-1} were fabricated using thin mono-crystalline silicon wafers as substrates. The measurements were made with a Pye Unicam spectrophotometer (model SP 2000) using an uncoated substrate to eliminate any possible influence of the substrate on the optical characteristics.

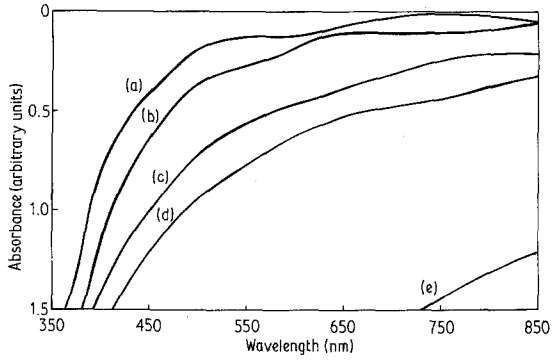

Figure 1 Absorption spectra of Mn–SiO thin film cermets. (a) 100 wt % SiO; (b) 95 wt % SiO, 5 wt % Mn; (c) 80 wt % SiO, 20 wt % SiO, 20 wt % Mn; (d) 78 wt % SiO, 22 wt % Mn; (e) 75 wt % SiO, 25 wt % Mn.

The annealing process was carried out at 250° C *in vacuo* ~ 5.0×10^{-4} Pa for 2 h and the specimen was then cooled to room temperature at a rate $< 3°$ C min^{-1}.

3. Results and discussion

3.1. Ultraviolet and visible

The ultraviolet and visible absorption spectra for cermet films of varying compositions, but fixed thickness of 300 nm, are presented in Fig. 1. The films were deposited at an R/P of 9.0×10^3 nm sec^{-1} Pa^{-1} and a substrate temperature of 20° C. It can be seen that as the manganese content of the films increases the fundamental absorption edge moves towards longer wavelengths. The graph of $\{\alpha(\omega)\hbar\omega\}^{1/2}$ against $\hbar\omega$ (Fig. 2) has a well-defined linear region, thus confirming that Equation 1 is obeyed; values of E_{opt} and B are given in Table I.

Fig. 3 demonstrates that the exponential behaviour of the absorption edge, via Equation 2, is satisfied in our cermet films. Values of the width E_e of the band-tails are also listed in Table I.

The origin of the exponential behaviour of $\alpha(\omega)$ on photon energy in both crystalline and amorphous semiconductors is still uncertain. Dow and Redfield [21] suggest that it arises from fluctuations in the internal fields associated with structural disorder in many amorphous solids. Tauc [22] says that it is a consequence of electronic transitions between localized states in the band-tails, the density of which is assumed to fall off exponentially with energy. Davis and Mott [3], on the other hand, have disputed Tauc's suggestion

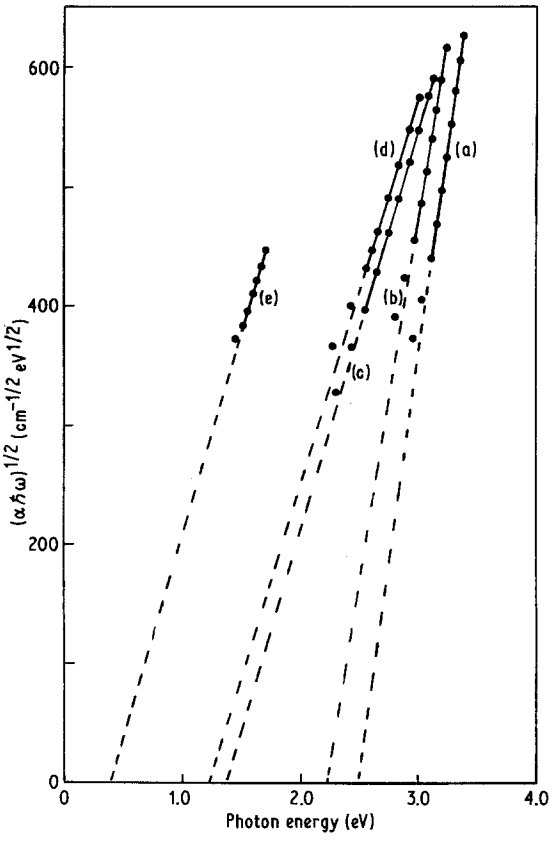

Figure 2 Data of Fig. 1 replotted in terms of indirect transitions.

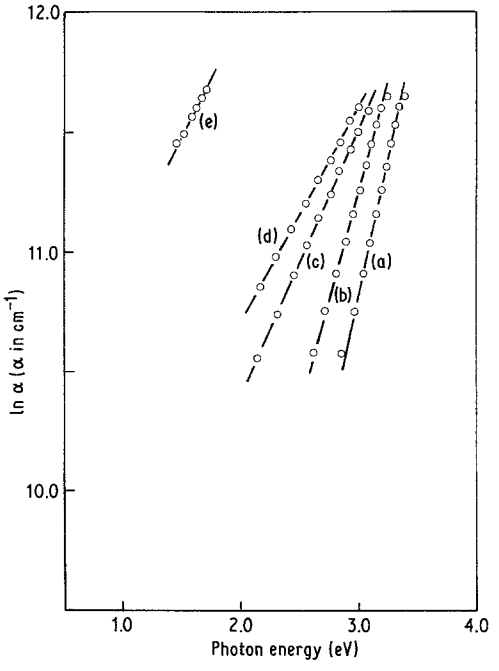

Figure 3 Data of Fig. 1 replotted in accordance with the Urbach law.

because the slopes of the observed absorption edges have roughly the same value (0.047 to 0.067 eV) for a wide variety of materials.

The exponential dependence of $\alpha(\omega)$ on $\hbar\omega$ for the cermet films indicates that they obey Urbach's rule. Also, as the values of E_e are very much larger than 0.05 eV and vary significantly with composition, Tauc's model based on electronic transitions between localized states in the band-edge tails may well be valid in our materials; an unambiguous interpretation of the nature of the absorption edge requires that the effect of temperature be considered. However, it is clear that the addition of manganese to SiO produces a reduction in E_{opt}. It may be noted that the room temperature d.c. activation energy for electrical conduction varies from 0.2 eV for 5 wt % Mn to 0.4 eV for 25 wt % Mn [23], values which are much less than $\frac{1}{2}E_{opt}$. Therefore, an impurity band must exist within the mobility gap, which determines both the activation energy and the carrier mobility.

Figs. 4 and 5 depict the variation of $\alpha(\omega)$ with $\hbar\omega$ for SiO_x films prepared at different values of R/P. An increase in R/P from 7.5×10^2 to 9.0×10^3 nm sec^{-1} Pa^{-1} produces a monotonic decrease in E_{opt} from 3.0 to 2.5 eV. The values of B given in Tables I to III are in good agreement with the theoretical values [1, 4]. It is expected that gaseous contamination of the films should decrease as R/P increases but that the number of unsatisfied bonds should increase [7].

TABLE I The optical properties of cermet films, 300 nm thick, deposited at 20° C and $R/P \sim 9.0 \times 10^3$ nm sec^{-1} Pa^{-1}

Cermet films composition (wt % SiO)	As-evaporated			After annealing		
	E_{opt} (eV)	E_e (eV)	B (10^5 cm^{-1} eV^{-1})	E_{opt} (eV)	E_e (eV)	B (10^5 cm^{-1} eV^{-1})
100	2.50	0.45	4.90	2.635	0.32	7.56
95	2.20	0.55	3.20	2.32	0.53	4.65
80	1.40	0.90	1.15	1.50	1.04	1.40
78	1.25	1.10	1.10	–	–	–
75	0.40	–	1.15	–	–	–

TABLE II Optical characteristics of SiO_x films, 300 nm thick, at 20° C

(R/P) (nm sec^{-1} Pa^{-1})	As-evaporated						After annealing		
	E_{opt} (eV)	E_e (eV)	B (10^5 cm^{-1} eV^{-1})	Infrared absorption peaks (cm^{-1})			E_{opt} (eV)	E_e (eV)	B (10^5 cm^{-1} eV^{-1})
1.15×10^3 [x]	3.05	0.507	3.08	1100	750	430	3.30	0.526	4.08
2.70×10^3 [y]	2.67	0.366	6.04	1080	750	400	2.66	0.366	4.90
9.0×10^3 [z]	2.50	0.450	4.90	1070	750	440	2.635	0.32	7.56

[x,y,z] Results shown in Figs. 4 and 5.

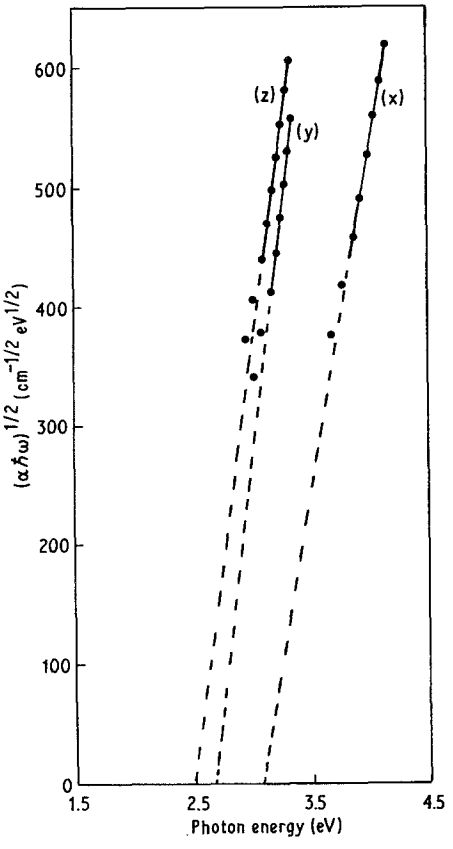

Figure 4 Optical data for SiO_x films deposited at different values of R/P (Table II).

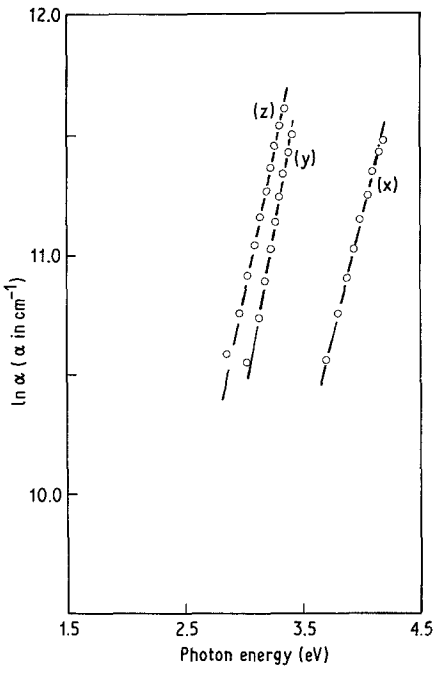

Figure 5 Data of Fig. 4 plotted in accordance with the Urbach law (Table II).

A 20 wt % Mn cermet has also been studied over the same range of R/P and the corresponding optical parameters are given in Table III. There is a systematic decrease in E_{opt} and an increase in E_e as R/P is increased.

The influence of substrate temperature on the optical parameters of SiO_x films is illustrated in Table IV. For a given wavelength, $\alpha(\omega)$ does not change appreciably with substrate temperature, and the change is even less pronounced as the degree of vacuum improves. Thus, in agreement with earlier findings [24], it seems that oxygen has a minor effect on film composition, and this conclusion finds support from the fixed position of the infrared absorption peaks in Table IV. The one exception occurs at a substrate temperature of 100° C, where the peaks shift towards higher wave numbers. The reason for this is uncertain at present.

Table V lists values of refractive index, n, estimated from Equation 5. As substrate temperature increases, the sticking coefficient for oxygen, the degree of oxidation and the density of voids should all decrease, leading to a more optically dense film and a higher refractive index.

The shapes of the absorption edges of some annealed SiO_x and cermet films display roughly the same characteristics as those of the unannealed films, but are shifted towards shorter wavelengths; at each R/P, E_{opt} and B increase as E_e decreases (Tables I and II). As explained elsewhere [7],

TABLE III Optical parameters for 20 wt % Mn cermet films (300 nm thick) deposited at room temperature at different R/P ratios

(R/P) (nm sec^{-1} Pa^{-1})	E_{opt} (eV)	E_e (eV)	B (10^5 cm^{-1} eV^{-1})
7.20×10^2	2.58	0.75	1.27
1.44×10^3	1.85	0.85	1.68
(1.44×10^3)*	1.98	1.13	1.27
9.0×10^3	1.40	0.92	1.14

*This specimen was immediately annealed *in vacuo* after the completion of the deposition process.

TABLE IV Optical parameters of SiO_x films (300 nm thick) deposited at an R/P of 9.0×10^3 nm sec^{-1} Pa^{-1}

Substrate temperature (° C)	As-evaporated						After annealing		
	E_{opt} (eV)	E_e (eV)	B (10^5 cm^{-1} eV^{-1})	Infrared absorption peaks (cm^{-1})			E_{opt} (eV)	E_e (eV)	B (10^5 cm^{-1} eV^{-1})
20	2.50	0.45	4.90	1070	750	440	2.635	0.32	7.56
20*				1050	750	420			
100	2.43	0.425	3.40	1090	830	450	2.65	0.373	4.92
200	2.40	0.38	4.90	1045	750	420	2.45	0.333	6.48
300	2.47	0.35	5.78	1060	760	430	2.55	0.32	7.24

*Specimen thickness ~ 1 μm

TABLE V Values of refractive index of Mn/SiO and SiO_x films

(a) For Mn/SiO cermet films deposited at 20° C

Cermet films composition (wt % SiO)	Specimen thickness (nm)	(R/P) (nm sec^{-1} Pa^{-1})	Refractive index	
			Unannealed value	Annealed value
95	300	9.0×10^3	3.62	3.70
95	690	3.0×10^3	2.98	–
80	300	7.5×10^2	3.03	2.98
80	442	7.5×10^2	2.70	–
80	610	7.5×10^2	2.85	–

(b) For SiO_x films

Specimen thickness (nm)	(R/P) (nm sec^{-1} Pa^{-1})	Substrate temperature (° C)	Refractive index
300	7.20×10^2	20	2.44
300	9.0×10^3	20	2.63
300	9.0×10^3	200	3.80
300	9.0×10^3	300	3.60
410	1.5×10^3	20	3.25
421	5.0×10^3	20	2.81
1050	1.05×10^4	20	2.65

during the annealing process the film relaxes to a lower energy configuration, the volume density of gaseous impurities and dangling bonds falls, bond lengths and angles redistribute themselves and E_{opt}, therefore, increases towards a limiting value, more nearly characteristic of the pure material.

3.2. Infrared

The infrared transmission spectra of SiO_x films prepared at various values of R/P and substrate temperatures are shown in Fig. 6. There is a strong band at 1050 cm^{-1} and moderately strong bands at 750 and 420 cm^{-1}. In the higher frequency region no absorption by SiOH groups was evident at 3650 cm^{-1} and by absorbed H_2O at 3400 cm^{-1}. Thus our SiO_x films have a low porosity.

The structure of SiO_x has been described by (a) the random bonding model, and (b) the mixture model. In the first, the non-stoichiometric SiO_x films are a single-phase system, consisting of a statistical mixture of fine randomly-bonded tetrahedra: $Si–(Si_yO_{4-y})$, where $0 \leqslant y \leqslant 4$ [25]. In (b) the films consist of a simple mixture of silicon and SiO_2. Evidence in support of (b) is that the absorption edge of the mixture ought to coincide with that of silicon, and be independent of composition. However, the monotonic shift in the optical absorption edge, shown in Fig. 4, indicates that this is not the case. This conclusion is also supported by the shift in the main infrared absorption peak at 1100 cm^{-1} (Fig. 6), which is characteristic of SiO_2. Table II confirms that a decrease of R/P is equivalent to x in SiO_x tending to the value 2. No Si_2O_3 is present in our films because there is no absorption band centred at 870 cm^{-1} [26].

Table II indicates a slight systematic decrease in the main infrared absorption peak as R/P increases, whereas Table IV shows that the varia-

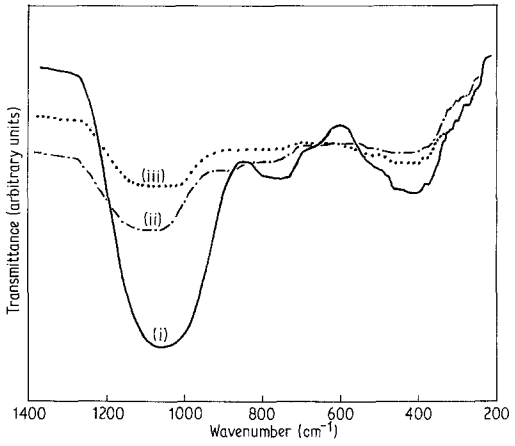

Figure 6 Infrared absorption spectra of three SiO_x specimens: (i) ~ 1050 nm thick, $R/P = 1.05 \times 10^4$ nm sec^{-1} Pa^{-1}; (ii) ~ 300 nm thick, $R/P = 1.15 \times 10^3$ nm sec^{-1} Pa^{-1}; (iii) ~ 300 nm thick, $R/P = 9.0 \times 10^3$ nm sec^{-1} Pa^{-1}.

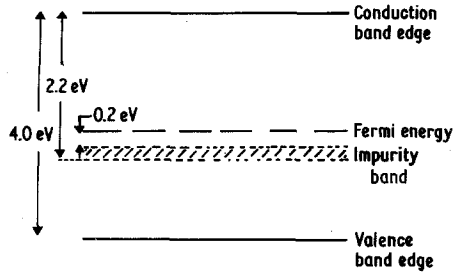

Figure 7 Possible energy band diagram for Mn–SiO cermet films.

tion with substrate temperature is more random. However, despite the high deposition rate of 6 nm sec^{-1} an absorption band in the vicinity of 1000 cm^{-1}, characteristic of true SiO films, [7, 27], was not obtained Owing to damage of the tantalum boat, it was not possible to use higher rates in our system.

The infrared absorption spectra of 5 and 22 wt % Mn cermet films at an R/P of 9.0×10^4 nm sec^{-1} Pa^{-1} display three bands centred at 1050, 750 and 450 cm^{-1}. These values are similar to those obtained at lower R/P ratios [23]. Thus we conclude that the absorption bands are characteristic of SiO_x, as well as there being evidence of chemical interaction between manganese and SiO_x.

4. Conclusion

In the light of the above discussion it is possible to suggest a tentative model of the electronic band structure in Mn/SiO cermet films, see Fig. 7. In doing so we assume that the Fermi level is roughly midway between the valence and conduction bands. The introduction of manganese into the SiO_x matrix gives rise to defects, which for the 5 wt % Mn cermet produces a narrow impurity band at about 0.2 eV below the Fermi energy. Combining knowledge of the activation energy with our estimate of the optical band gap we obtain a value of 4.0 eV for the mobility band gap. It should perhaps be noted that an impurity band lying at 1.65 eVabove the valence band has been observed in GeO_2 glass [28].

Acknowledgements

We should like to thank Dr D. N. Waters of the Department of Chemistry for use of the spectrophotometers. ARS wishes to thank The Association of Commonwealth Universities for the award of a Commonwealth Scholarship and SKJAA the Ministry of Higher Education and Scientific Research in Iraq for the award of a scholarship.

References

1. J. TAUC, "Amorphous and Liquid Semiconductors" (Plenum Press, London, 1974) p. 159.
2. J. TAUC, R. GRIGOROVICI and A. VANCU, *Phys. Status Solidi* **15** (1966) 627.
3. E. A. DAVIS and N. F. MOTT, *Phil. Mag.* **22** (1970) 903.
4. N. F. MOTT and E. A. DAVIS, "Electronic Processes In Non-crystalline Materials" (Clarendon Press, Oxford, 1979) pp. 291, 497.
5. G. R. MORIDI and C. A. HOGARTH, Proceedings 7th International Conference on Amorphous and Liquid Semiconductors (Edinburgh) (1977) edited by W. E. Spear (Centre for Industrial Consultancy, Edinburgh) p. 688.
6. C. A. HOGARTH and M. Y. NADEEM, *Phys. Status Solidi (2)* **68** (1981) K181.
7. S. K. J. AL-ANI, K. ARSHAK and C. A. HOGARTH, *J. Mater. Sci.* **19** (1984) 1737.
8. F. URBACH, *Phys. Rev.* **92** (1953) 1324.
9. J. E. MORRIS and T. J. COUTTS, *Thin Solid Films* **47** (1977) 1.
10. Z. H. MEIKSIN, *Phys. Thin Films* 8 (1975) 99.
11. B. ABELES, PING SHENG, M. D. COUTTS and Y. ARIE, *Adv. Phys.* **24** (1976) 407.
12. A. A. MILGRAM and C. S. LU, *J. Appl. Phys.* **39** (1968) 4219.
13. R. GLANG, R. A. HOLMWOOD and S. R. HERD, *J. Vac. Sci. Technol.* 4 (1967) 163.
14. J. E. MORRIS, *Thin Solid Films* **11** (1972) 299.
15. J. K. POLLARD, R. L. BELL and G. G. BLOODSWORTH, *J. Vac. Sci. Technol.* 6 (1969) 702.
16. E. M. CASTRO and J. BEYNON, *Thin Solid Films* **66** (1980) L19.
17. *Idem, ibid.* **66** (1980) L21.
18. *Idem, ibid.* **69** (1980) L21.
19. *Idem, ibid.* **69** (1980) L43.
20. T. S. MOSS, G. J. BURRELL and B. ELLIS, "Semiconductor Opto-electronics" (Butterworth, 1973) 18.
21. J. D. DOW and D. REDFIELD, *Phys. Rev.* **B5** (1972) 594.
22. J. TAUC, "The Optical Properties of Solida", edited by F. Abeles (North Holland, Amsterdam, 1970) p. 277.
23. A. R. SARKAR, unpublished results.
24. A. P. BRADFORD, G. HASS, M. McFARLAND and E. RITTER, *Thin Solid Films* **42** (1977) 361.
25. H. R. PHILIPP, *J. Phys. Chem. Solids* **32** (1971) 1935.
26. A. L. SHABALOV and M. S. FELDMAN, *Thin Solid Films* **110** (1983) 215.
27. E. RITTER, *Opt. Acta* 9 (1962) 197.
28. M. N. KHAN and E. E. KHAWAJA, *Phys. Status Solidi (a)* **74** (1982) 273.

Received 5 April
and accepted 23 May 1984